Plasma Chemical Study of a RF Discharge Containing Aluminum Tri-Isopropoxide Using MIR Absorption Spectroscopy Based on External-Cavity Quantum Cascade Lasers

D. Lopatik[1], **S. Niemietz**[2], **M. Fröhlich**[2], **J. Röpcke**[1]*, and **H. Kersten**[2]

[1] Leibniz Institute for Plasma Science and Technology e.V. (INP), Felix-Hausdorff-Str. 2, 17489 Greifswald, Germany

[2] Institute of Experimental and Applied Physics, University of Kiel, Leibnizstr. 19, 24098 Kiel, Germany

In Ar and Ar/N_2 RF plasmas with admixtures of aluminum tri-isopropoxide (ATI) the fragmentation of this metal-organic precursor has been studied by means of infrared absorption spectroscopy (IR-AS) using an external-cavity quantum cascade laser (EC-QCL) arrangement. The experiments were performed in an asymmetric capacitively coupled reactor at a frequency of f = 13.56 MHz and a pressure of up to p = 10 Pa. The discharge power was in the range of P = 40 – 100 W. Using EC-QCLAS the evolution of the concentrations of six stable molecules, CH_4, C_2H_2, C_2H_4, H_2O, HCN and HNO_3, has been monitored in the plasma. The concentrations of these plasma chemical products were found to be in the range of about $7\times10^{12} - 2\times10^{14}$ molecules cm^{-3}.

1 Introduction

Metal organic precursors are frequently used in plasma processes for the deposition of metal oxide layers. The advantage of these precursors is that they have a relatively low boiling point and, thus, they can easily be inserted into a plasma. Typical precursors for plasma-enhanced chemical vapor deposition (PECVD) include for example silane [1], hexamethyldisiloxane (HMDSO) [2,3] and aluminum tri-isopropoxide (ATI). In contrast to silicon-based precursors, which have been widely studied in plasmas, only a few publications exist about the usage of aluminum-based precursors [4]. Already in the late 1960's Daasch et al. made first investigations on ATI. However, these investigations were not performed under plasma conditions. They used mass spectrometry to determine the components of hot ATI gas. One of their results was, that ATI consists of different types of species with the formula $(Al(OC_3H_7)_3)_x$, where x ranges from 1 to 7. For illustration, in figure 1 the monomeric and tetrameric structure of ATI is shown.

Solid ATI was studied by Folting et al. in the 1990's [6] and by Turuva et al. already in 1979 [7]. They carried out X-ray diffraction to determine crystal structure and bond lengths. An important use of ATI is for the deposition of Al_xO_y layers in CVD processes [8]. For example, cutting tools are coated with Al_xO_y layers. These layers show high hardness, chemical resistance and low thermal conductivity, which is needed for high performance cutting applications [9]. Another example for alumina deposition is the use as diffusion barrier. These barriers are needed for the production of OLED devices to prevent permeation of O_2 and H_2O through the flexible plastic substrates [10]. ATI also shows catalytic effects in chemical processes, for example for the co-polymerization of cyclohexene oxide with CO_2 [11].

In the past properties of Al_xO_y layers have been studied using different methods. In the 1980's Saraie et al. measured the deposition rate of Al_xO_y layers in CVD processes in dependence on the substrate temperature and on the source gas supply by multi-interference microscopy [12]. Huntz and co-workers made in situ investigations

---

* Corresponding author. E-mail: roepcke@inp-greifswald.de

Fig. 1 a) Monomeric and b) tetrameric ATI.

on growing layers using X-ray diffraction and scanning electron microscopy [13]. They also investigated the transformations occurring in Al_xO_y layers during heat-treatment. Long-term stability of the deposited alumina layers is an important issue. The investigations of Sovar et al. showed that despite the ageing of ATI, it can be used principally for depositing stable Al_xO_y layers [14]. For high temperature applications also mixed structures were used. For example, Al_xO_y and SiO_x layers were deposited on polyimide composites for thermo-oxidative protection. These coatings improved the stability of polyimide composites at elevated temperatures [15].

Although ATI containing plasmas are used for deposition in PECVD processes [16] the chemical reactions are far from being completely understood in these plasmas. In discharges containing ATI for an analysis of chemical phenomena information about the absolute ground state concentration of molecular precursors, fragments and products including transient species like radicals in relation to the discharge parameters as e.g. gas mixture and power would be very helpful.

Tunable diode laser absorption spectroscopy (TDLAS) in the mid-infrared spectral range using lead salt lasers as radiation sources has been proven to be a versatile diagnostic technique of molecular gases and plasmas. In particular TDLAS is well suited for the measurement of absolute ground state concentrations of a wide variety of molecular species including radicals and molecular ions thereby providing a link with chemical modelling of the plasma (see [17] and references therein). Until now, the main applications of TDLAS have been for investigating molecules and radicals in fluorocarbon etching plasmas [38] and in plasma containing hydrocarbons [17]. For the simultaneous monitoring of multiple molecular plasma species TDLAS systems, which make use of several lead salt lasers, have been developed in the past [18,19]. In contrast to ATI the plasma based fragmentation of other precursors, as silane and HMDSO, has been already investigated in several TDLAS studies, e.g. [20,21].

The recent development and commercial availability of pulsed and continuous wave quantum cascade lasers (QCLs) for wavelengths longer than 3.4 μm and inter-band cascade lasers (ICLs) for shorter wavelength offer an attractive new option for mid-infrared laser absorption spectroscopy (MIR-LAS) for plasma diagnostic purposes. Distributed feedback (DFB) QCLs provide continuous mode-hop free wavelength tuning. Their total emission range is typically limited to less than $7 \, cm^{-1}$. Therefore, a multi-component detection to study infrared active compounds in reactive plasmas requires, as in the TDLAS case, the combination of several QCLs in a spectrometer [22]. Meanwhile the variety of QCLs and ICLs operating at room temperature are considered as substitutes for cryogenic cooled lead salt lasers, which has led to a rapid development of MIR-LAS from a niche position to a standard diagnostic technique [23], even for the study of metal-organic precursor fragmentation, as silane and HMDSO, and also of fluorcarbons in plasmas [24,25,39].

Recently, tunability over much broader spectral ranges than with a typical lead salt lasers or DFB-QCL has been achieved using external cavity (EC) configurations. Nowadays, EC-QCL, which are available in pulsed or continuous (cw) wave working mode, can be tuned over more than $100 \, cm^{-1}$. Modern cw EC-QCL provide mode-hop free tuning ranges in the order of up to $80 \, cm^{-1}$, at small line width of typically 20 to 60 MHz (6 – $18 \times 10^{-4} \, cm^{-1}$) at power values of up to 150 mW [26]. At present EC-QCLs are used for an increasing number of applications including high resolution isotope analysis, trace gas monitoring and explosive detection [27-29]. Recently, cw EC-QCLs have been tested as radiation sources for MIR-LAS studies of molecular plasmas [30].

In the presented investigation chemical phenomena of Ar and Ar/N_2 RF discharges containing ATI as metal-organic precursor have been in the focus of interest. Using MIR-LAS based on a cw EC-QCL arrangement the evolution of the concentrations of six stable molecules, CH_4, C_2H_2, C_2H_4, H_2O, HCN and HNO_3, has

been monitored in the plasma. One of the objectives was to determine main fragmentation pathways of the ATI precursor molecule and to receive information about the influence of added rare and molecular gases, as e.g. Ar and Ar/N_2.

2 Experimental

The investigations have been performed in an asymmetric capacitively coupled RF discharge at a frequency of f = 13.56 MHz. The vacuum chamber with a volume of about 50 dm^3 is cylindrical with a plain electrode and several ports for diagnostics approaches. The used RF generator was a CESAR\TM 133 from Advanced Energy Industries. The vacuum chamber was evacuated by a turbo pump (Varian Turbo-V 301) and a roughing pump (Varian IDP3 scroll pump). The pressure was measured by a pirani and a baratron vacuum meter. As shown in the scheme of the experimental setup in figure 2, on the top of the chamber the gas inlet for carrier and reactive gas is located. As carrier gas argon (99.999%) and nitrogen (99.999%) and as metal-organic precursor ATI were used. The measurements were performed at pressure values of up to p = 10 Pa and at discharge power values in the range of P = 40 – 100 W. To keep the total pressure constant, the Ar and N_2 gas flows were adjusted manually by a needle valve and the ATI gas flow by a viscometer. The ATI vapor was provided by a special designed heating system. The turbo-molecular pump has a throughput of 1 mbar s^{-1} at the operating pressure, leading to a residence time of about 1s for the incoming gas flow.
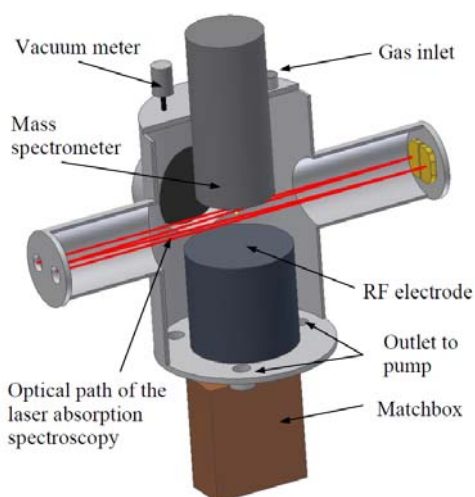
Fig. 2 Experimental arrangement of the RF plasma reactor
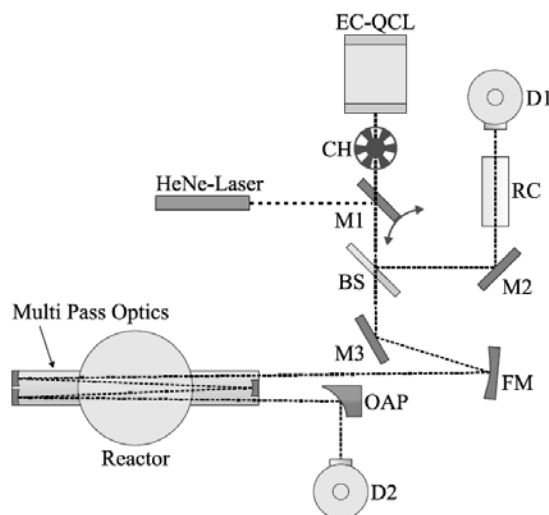
Fig. 3 Scheme of the EC-QCLAS spectrometer in combination with the RF plasma reactor. (CH: chopper, M1-M3: mirrors, BS: beam splitter, RC: reference gas cell, D1, D2: HgCdTe detectors, FM: focal mirror, OAP: out of axis paraboloid).

By variation of one of the parameters, (i) discharge power, (ii) total pressure or (iii) gas mixture, molecular concentrations of generated stable molecular species, CH_4, C_2H_2, C_2H_4, H_2O, HCN and HNO_3, were measured by an EC-QCL absorption spectrometer. The scheme of the spectrometer is given in figure 3. The set-up consists (i) of the radiation source, an EC-QCL, Daylight Solution, with a full tuning possibility in the range of 1305 to 1445 cm^{-1}, providing a mode hop free range between 1345 and 1400 cm^{-1} at a maximum power of about 150 mW, (ii) a chopper, (iii) two standard HgCdTe detectors for measuring and reference path and (iv) opto-mechanical elements for beam guiding. Further details can be found in ref. [30]. The infrared laser beam from the EC-QCL system has a diameter of about 1 cm and is transferred using gold-coated mirrors via KBr-windows to an optical long path cell (White cell type [31], 20 passes, absorption length: 15.8 m), which is mounted to the plasma chamber for improved sensitivity (figure 2). The diode laser beam leaving the cell was focused on a standard HgCdTe infrared detector by an off-axis parabolic mirror. The identification of lines and the determination of their absolute positions were carried out using well-documented reference gas spectra and

an etalon of known free spectral range for interpolation. Spectral positions and absorption line strengths of molecular ground state absorption lines used for the measurements are listed in Table 1.

The used data acquisition method is an advanced form of sweep integration which is carried out based on the software package TDLWintel [18].

Table 1 Species, spectral positions and line strengths used for the EC-QCLAS measurements [32].

Species	Spectral position [cm^{-1}]	Absorption line strength [cm^{-1}/(molecule cm^{-2})]
CH_4	1332.731	9.557E-20
C_2H_2	1332.803	4.583E-20
C_2H_4	1413.212	5.645E-21
H_2O	1375.086	1.490E-20
HCN	1382.514	4.408E-20
HNO_3	1332.891	1.530E-20

Absolute species concentrations are returned from the nonlinear least-squares fits of the measured absorption features so that external calibration is not required. For the calculations of the concentrations a gas temperature of 300 K was used since this is a good average for the gas temperature over the line of sight, comprising the active zone over the discharge electrode and the afterglow surrounding them, and over the course of the measurement.

Figure 4 shows an exemplary spectrum of CH_4, C_2H_2 and HNO_3 absorption lines in an Ar/N$_2$/ATI plasma.
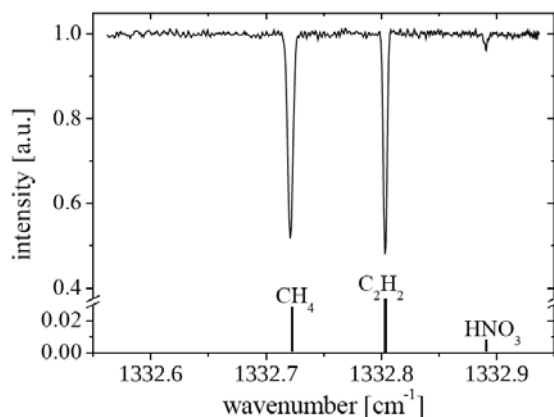
Fig. 4 Exemplary spectrum of of CH_4, C_2H_2 and HNO_3 absorption lines in an Ar/N$_2$/ATI plasma

3 Results and Discussion

The plasma chemical study of the ATI fragmentation in the RF plasma has been performed for two different conditions of the gas mixture, i.e. case 1: within a pure ATI-Ar mixture and case 2: using a ATI-N$_2$-Ar feed gas. In figures 5-7 the experimental results for the ATI-Ar case are given.

Some useful generalizations follow from these figures. The concentrations of the plasma chemical products, CH_4, C_2H_2, C_2H_4 and H_2O, were found to be in the range of about $7\times10^{12} - 2\times10^{14}$ molecules cm^{-3}. Plasma dissociation of the ATI precursor molecules leads not only to AlO_x fragments but also to a relatively high density of methyl (CH_3) groups and hydrogen [33]. The methyl radicals can directly react with hydrogen to methane (CH_4):

$$CH_3 + H \rightarrow CH_4 \tag{1}$$

In a plasma environment also acetylene as well as ethylene are formed by two methyl groups, see formula (2) and (3) [34,35].

$$CH_3 + CH_3 \rightarrow C_2H_2 + 4H \tag{2}$$

$$CH_3 + CH_3 \rightarrow C_2H_4 + 2H \tag{3}$$
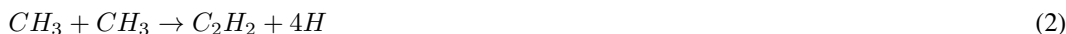
The largest of the hydrocarbon product molecules, C_2H_4, shows the lowest concentration, while acetylene is appearing with the highest density. For methane intermediate values could be monitored. It is interesting to note, that the concentrations of C_2H_2 and C_2H_4 decrease with power, while the methane concentration remains nearly constant, see figure 5. This behaviour may be caused by the increasing degree of dissociation with power not only of the ATI precursor molecule, but also of the higher hydrocarbon products. Hydrogen can be dissociated from C_2H_2 or C_2H_4 by electron collisions [36,37]:

$$C_2H_2 + e^- \rightarrow C_2H + H + e^- \tag{4}$$

$$C_2H_4 + e^- \rightarrow C_2H_3 + H + e^- \tag{5}$$
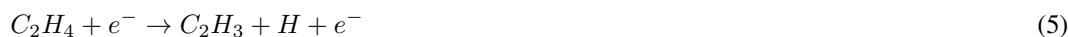
The enhanced dissociation is caused by an increased collision rate of electrons and molecules due to higher electron density with increasing RF power [33].
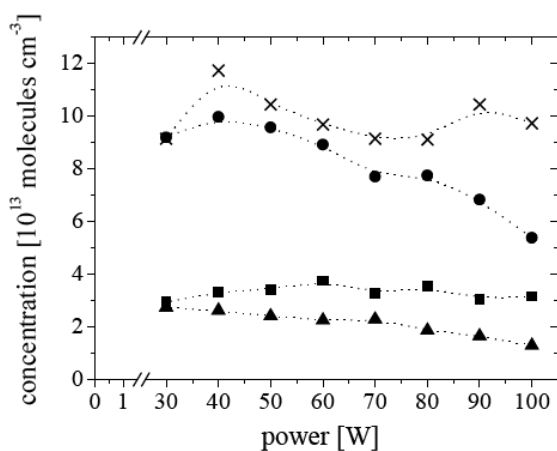
Fig. 5 Concentration of CH_4 - ■, C_2H_2 - ●, C_2H_4 - ▲ and H_2O - × in dependence on the discharge power in an Ar/ATI plasma, p = 6 Pa, ratio Ar/ATI=2/1.
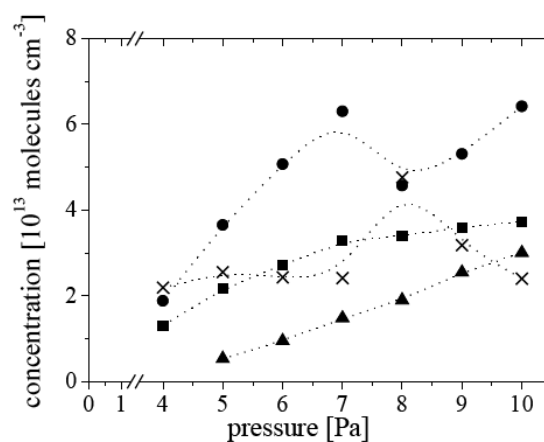
Fig. 6 Concentration of CH_4 - ■, C_2H_2 - ●, C_2H_4 - ▲ and H_2O - × in dependence on the pressure in an Ar/ATI plasma P = 80 W, ratio Ar/ATI=2/1.
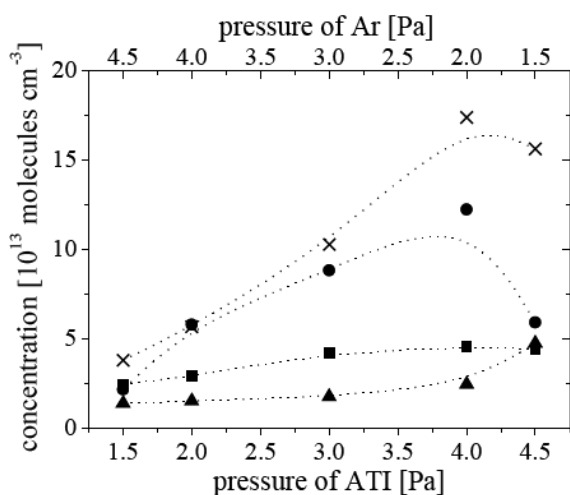
Fig. 7 Concentration of CH_4 - ■, C_2H_2 - ●, C_2H_4 - ▲ and H_2O - × in dependence on the mixing ratio of Ar to ATI, given in pressure values, in an Ar/ATI plasma, p = 6 Pa, P = 80 W.

As expected the concentration of all four molecular species increases with increasing pressure, see figure 6. A comparable behaviour is observed, in case the total pressure remained constant and only the ATI partial pressure has been varied as shown in figure 7. This observation indicates that the increasing ATI pressure results in a higher concentration of fragmentation products.

In all of these three experiments the water concentration was found to be on a comparable high value, reaching a maximal value of 2×10^{14} molecules cm^{-3} at high ATI admixture (figure 7). In general the detected water can originate from two different sources, (i) from the plasma chemical conversion of ATI and (ii) from residual water inside the reactor, in particular, adsorbed at the reactor walls. From the present experimental results, it is difficult to distinguish between these two sources. However, one could speculate that the main source is the ATI precursor itself, because the amount of water is nearly constant for a constant ATI admixture (figures 5 and 6) but it is increasing at higher ATI admixture (figure 7).

For the second experimental situation, case 2, nitrogen was used additionally as feed gas component. In the available spectral range of the used EC-QCL two other additional molecular species could be identified, HCN and HNO$_3$. These molecules are certainly generated by reactions of ATI fragmentation products with nitrogen. The results of the plasma chemical QCLAS study are shown in figures 8 and 9.
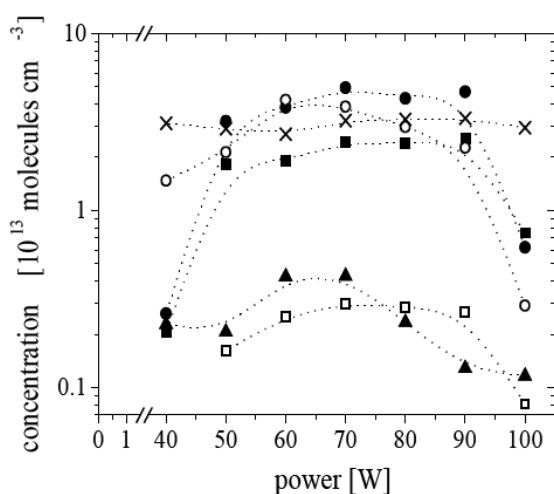
Fig. 8 Concentration of CH$_4$ - ■, C$_2$H$_2$ - •, C$_2$H$_4$ - ▲ H$_2$O - ×, HCN - ○ and HNO$_3$ - □ in dependence on the discharge power in an Ar/N$_2$/ATI plasma, p = 6 Pa, ratio Ar/N$_2$/ATI=1/1/1.
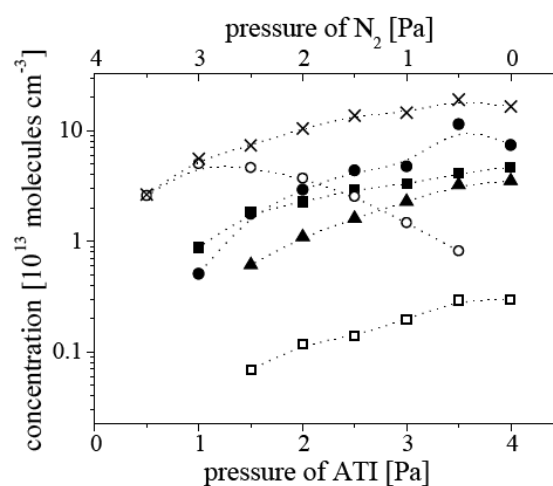
Fig. 9 Concentration of CH$_4$ - ■, C$_2$H$_2$ - •, C$_2$H$_4$ - ▲ H$_2$O - ×, HCN - ○ and HNO$_3$ - □ in dependence on the mixing ratio of N$_2$ to ATI, given in pressure values, in an Ar/N$_2$/ATI plasma, p = 6 Pa, p$_{Ar}$= 2 Pa, P = 80 W.

In figure 8 the concentration of six observable product molecules, CH$_4$, C$_2$H$_2$, C$_2$H$_4$, H$_2$O, HCN and HNO$_3$, in dependence on the discharge power in an Ar/N$_2$/ATI plasma with a mixing ratio of 1/1/1 at a total pressure of p = 6 Pa are given. It is interesting to note, that the concentrations of all molecules, except water, show a maximum at medium power values between 50 and 90 W. The decrease of concentration above 90 W may be explained by more effective collisions of electrons with nitrogen molecules, finally leading to a limited fragmentation of ATI. The maximum concentration was found for C$_2$H$_2$ to be about 5×10^{13} molecules cm^{-3}, followed by HCN, H$_2$O and CH$_4$. A second group of molecular species is formed by C$_2$H$_4$ and HNO$_3$ with concentrations of about one order of magnitude lower than the species of the former group.

With increasing admixture of ATI compared to the nitrogen partial pressure again most of the molecules show increasing concentrations except HCN (figure 9). For the concentration of HCN a slight maximum was found at an ATI admixture of about 1 Pa. The concentration of HNO$_3$ was again in the range of 10^{12} molecules cm^{-3}. The coupled process of decreasing nitrogen pressure and increasing ATI concentration makes it difficult to give an explanation about the formation of HCN and HNO$_3$ regarding the fragmentation process and the chemical reactions of the products with nitrogen. But it seems to be obvious that the different electron collision cross sections for ATI and N$_2$ dissociation are the reason for this behavior, e.g. the importance of different reaction channels in dependence on the plasma process conditions causes the observed changes. Even the Ar-N$_2$ mixing ratio can have a considerable influence on the dissociation behavior of the molecular feed gases, as described by Saloum and co-workers [41].

4   Summary and conclusions

In the present study the absolute ground state concentrations of six stable species under a wide range of experimental conditions have been determined by infrared laser absorption spectroscopy providing a link with the fragmentation behaviour of ATI in a capacitively coupled RF discharge. The final objective to get a better understanding of chemical processes occurring in plasmas containing metal-organic precursors for metal oxide PECVD deposition can be achieved by applying this method. Although several molecular species concentrations have been monitored in absolute scale, the mass balance of the whole ATI fragmentation process is far to be comprehensively analysed. Future studies should include (i) the ATI precursor molecule itself, (ii) further stable, in particular higher hydrocarbon molecules as well as other important intermediates, but also (iii) a quantitative analysis of the molecular production rates in the discharge. Especially, other radicals, as for example CH_3, C_2H, CH_2, CH and metal-organic species should be monitored. Further, the combination of infrared absorption with mass-spectrometric techniques, see ref. [33] where the complex fragmentation of the ATI molecule were studied recently, could lead to an optimization of deposition processes and to an improved modelling potential for ATI containing plasmas based on kinetic data as e.g. reliable reaction rates.

It has been shown, that based on the attractive properties of EC-QCLS, as in particular (i) wide spectral tunability, (ii) intrinsic narrow linewidth, and (iii) high output powers, this radiation source for absorption spectroscopy has a high potential to be applied for other plasma diagnostic purposes. In particular EC-QCLAS is well suited for the monitoring of multiple species including larger plasma components characterized by broader spectral features and also to be used under atmospheric pressure conditions, where pressure broadening effects have to be considered [40]. Further interesting fields like the kinetics of oxygen containing electronegative plasmas and also phenomena of plasma surface interaction should be accessible using these new MIR radiation sources.

References

[1] K. Bhattacharya and D. Das, Nanotechnology 18, 415704 (2007).
[2] M. Hähnel, V. Brüser, and H. Kersten, Plasma Process. Polym. **6**, 629 (2007).
[3] S. Bornholdt, M. Wolter, and H. Kersten, Eur. Phys. J. D **60**, 653 (2010).
[4] H. Kersten, G. Thieme, M. Fröhlich, D. Bojic, D.H. Tung, M. Quaas, H. Wulff, and R. Hippler, Pure Appl. Chem. **77**, 415 (2005).
[5] L. Daasch and H. Fales, Organic Mass Spectr. **2**, 1043 (1969).
[6] K. Folting, K.E. Streib, K.G. Caulton, O. Poncelet, and L.G. Hubert-Pfalzgraf, Polyhedron **10**, 1639 (1991).
[7] N.Y. Turova, V.A. Kozunov, A.I. Yanovskii, N.G. Bokii, Y.T. Struchkov, and B.L. Tarnopolskii,, J. Inorg. Nuclear Chem. **41**, 5(1979).
[8] S. Blittersdorf, N. Bahlawane, K. Kohse-Höinghaus, B. Atakan, and J. Muller, Chemical Vapor Dep. **9**, 194 (2003).
[9] M. Kathrein, W. Schintlmeister, W. Wallgram, and U. Schleinkofer, Surf. Coat. Technol. **163-164**, 181 (2003).
[10] M.D. Groner, S.M. George, R.S. McLean, and P.F. Garcia, Appl. Phys. Lett. **88**, 051907(2006).
[11] T.A. Zevaco, A. Janssen, J., Sypien, and E. Dinjus, Green Chem. **7**, 659-666 (2005).
[12] I. Saraie, J. Kwon, Y. Yodogawa, J. Electrochem. Soc. **132**, 890 (1985).
[13] A.M. Huntz, M. Andrieux, C. Vahlas, M.M. Sovar, D. Samelor, and A.N. Gleizes, J. Electrochem. Soc.**154**, 63 (2007).
[14] M.M. Sovar, D. Samelor, A. Gleizes, and C. Vahlas, Surf. Coat. Technol. **201**, 9159 (2007).
[15] L.M. Miller and D.A. Gulino, Surf. Coat. Technol. **68-69**, 76 (1994).
[16] H. Kersten, R. Wiese, G. Thieme, M. Fröhlich, A. Kopitov, D. Bojic, F. Scholze, H. Neumann, M. Quaas, H. Wulff, and R. Hippler, New J. Phys. **5**, 93.1 (2003).
[17] J.Röpcke, G. Lombardi, A. Rousseau, and P.B. Davies, Plasma Sources Sci. Technol. **15**, S148 (2006).
[18] J. Röpcke, L. Mechold, M. Käning, J. Anders, F.G. Wienhold, D. Nelson, and M. Zahniser, Rev. Sci. Instrum. **71**, 3706 (2000).
[19] J.B. McManus, D. Nelson, M. Zahniser, L. Mechold, M. Osiac, J. Röpcke, and A. Rousseau, Rev. Sci. Instrum. **74**, 2709 (2003).
[20] C. Yamada and E. Hirota, Phys. Rev. Lett. **56**, 923 (1986).
[21] J. Röpcke, G. Revalde, M. Osiac, K. Li, and J. Meichsner, Plasma Chem. Plasma Process. **22**, 139 (2002).
[22] M. Hübner, S. Welzel, D. Marinov, O. Guaitella, S. Glitsch, A. Rousseau, and J. Röpcke, Rev. Sci. Instr. **82**, 093102 (2011).

[23] S. Welzel, F. Hempel, M. Hübner, N.P. Lang, P.B. Davies, and J. Röpcke, Sensors **10**, 6861 (2010).
[24] R. Bartlome, A. Feltrin, and C. Ballif, Appl. Phys. Lett. **94**, 201501 (2009).
[25] M. Wolter, M. Hundt, and H. Kersten, Vacuum **85**, 482 (2010).
[26] R.F. Curl, F. Capasso, C. Gmachl, A.A. Kostorev, B. McManus, R. Lewicki, M. Pusharsky, G. Wysocki, and F.K. Tittel, Chem. Phys. Lett. **487**, 1 (2010).
[27] R.J. Walker, J.H. van Helden, and G.A.D. Richie, Chem. Phys. Lett. **501**, 20 (2010).
[28] A. Karpf and G.N. Rao, Appl. Optics **49**, 1406 (2010).
[29] R. Furstenberg, C.A. Kendziora, J. Stepnowski, S.V. Stepnowski, M. Rake, M.R. Papantonakis, V. Nguyen, G.K. Hubler, and R.A. McGill, Appl. Phys. Lett. **93**, 224103 (2008).
[30] D. Lopatik, N. Lang, U. Macherius, H. Zimmermann, and J. Röpcke, Meas. Sci. Technol. 2012, submitted.
[31] J.U. White, J. Optical Soc. America **32**, 285 (1942).
[32] L.S. Rothman, D. Jacquemart, A. Barbe, D.C. Benner, M. Birk, L.R. Brown, M.R. Carleer, C. Chackerian, K. Chance, L.H. Coudert, V. Dana, V.M. Devi, J.M. Flaud, R.R. Gamache, A. Goldman, J.M. Hartmann, K.W. Jucks, A.G. Maki, J.Y. Mandin, S.T. Massie, J. Orphal, A. Perrin, C.P. Rinsland, M.A.H. Smith, J. Tennyson, R.N. Tolchenov, R.A. Toth, J. Vander Auwera, P. Varanasi, and G. Wagner, J. Quant. Spectrosc. Radiat. Transfer **96**, 139 (2005).
[33] S. Niemietz, M. Fröhlich, and H. Kersten, Plasma Process. Polym. (2012) DOI:10.1002/ppap.201200012.
[34] M. Masi, C. Cavallotti, and S. Carra, Chemical Engineering Sci. **53**, 3875 (1998).
[35] K. Bleecker, A. Bogaerts, W. Goedheer, and R. Gijbels, IEEE Trans. Plasma Sci. **32**, 691 (2004).
[36] M. Hundt, P. Sadler, I . Levchenko, M. Wolter, H. Kersten, and K. Ostrikov, J. Appl. Phys. **109**, 123305 (2011).
[37] E. Kovacevic, I. Stefanovi, J. Berndt, and J. Winter, J. Appl. Phys. **93**, 2924 (2003).
[38] S. Stepanov and J. Meichsner, Plasma Sources Sci. Technol. **21**, 024008 (2012)
[39] S. Welzel, S. Stepanov, J. Meichsner, and J. Röpcke, J. Phys. D: Appl. Phys. **43**, 124014 (2010)
[40] S. Reuter, J. Winter, S. Iseni, S. Peters, A. Schmidt-Bleker, M. Dünnbier, J. Schäfer, R. Foest, and K.-D. Weltmann, Plasma Sources Sci. Technol. **21**, 034015 (2012).
[41] S. Saloum, M. Naddaf, and B. Alkhaled, J. Phys. D: Appl. Phys. **41**, 045205 (2008).